Journal of Ovonic Research Vol. 9, No. 2, March - April 2013, p. 35 - 43

EFFECTS OF PRECURSOR CONCENTRATION ON THE OPTICAL AND STRUCTURAL PROPERTIES OF Fe_2O_3 THIN FILMS SYNTHESIZED IN A POLYMER MATRIX BY CHEMICAL BATH DEPOSITION

A.B.C EKWEALOR*, F.I. EZEMA
Department of Physics and Astronomy, University of Nigeria, Nsukka

Fe_xO_y, thin films synthesized in the pores of PVP by chemical bath deposition techniques were deposited on glass substrates and characterized. For structural characterization, the films were subjected to x-ray diffraction (XRD), in the range of scanning angle 2θ with Cukα radiation (λ = 1.5406Å) using Philips .P.W 1500 X-ray diffractometer. The optical properties of the films were studied using absorption spectra in UV – VIS – NIR region obtained from Unico UV – 2102 PC spectrophotometer at normal incidence of light within the wavelength range 200nm – 1200nm. The synthesized Fe_xO_y films, were observed from XRD to be actually Maghemite, iron oxide, γ-Fe_2O_3, nanocrystals of size 55.76nm; this size however decreased to 22.44nm when the precursor concentration was increased. For these films, the transmittance (42% – 97%) of radiation was high for UV-VIS-NIR regions, but the absorbance (2% – 35%) and reflectance (2% – 20%) of radiation in these regions were low. The films had low band-gap of 2.14eV for low precursor concentration, and high band-gap of 2.95eV for high precursor concentration.

(Received December 14, 2012; Accepted March 5, 2013)

Keywords: Iron oxide, thin films, CBD, concentration, band gap and optical properties.

1. Introduction

Fe and O can form as many as 15 phases of oxides of iron [1]. These oxides are abundant in the earth's crust, and can be synthesized in pure or mixed oxides. Thin films of iron oxide have attracted considerable attention in last few years due to their interesting magnetic properties. [2]. Iron oxide films can be used in a wide range of applications. Properties, such as high refractive index, wide bandgap and chemical stability make them suitable for use as gas-sensors [3]. Iron oxide is known to have interesting properties as a photoanode [4, 5]. Moreover, it has been reported that thin films of iron oxide have higher photoenergy conversion efficiencies than those of the electrodes normally used [6]. The most common oxides are hematite (α-Fe_2O_3), maghemite (γ-Fe_2O_3) and magnetite (Fe_3O_4). These have different electrical, magnetic, electro-optical and chemical properties. Amongst these three common iron oxides hematite and maghemite have applications in gas sensors. Hematite is well known for its property of parasitic or canted magnetism. It is used in red pigments [7]; and has been tested as an electrode in photoelectrochemical (PEC) cell for energy conversion due to proper band gap [8]. Maghemite (γ-Fe_2O_3) is used in high-density magnetic recording devices [9]. Magnetite (Fe_3O_4) in different forms is well understood for its giant magnetoresistance. Nanoparticles of iron oxide, in its different phases are being currently under study due to their wide range of applications in various fields of cutting edge science and technology, like optoelectronics, solar cell window material, magnetic storage medium, catalysis, thin film electrodes for lithium-ion batteries, sensors, removal of heavy toxic metals like arsenic and in biomedical sciences, etc [10]. Numerous works have been

* Corresponding author: abcekwealor@yahoo.com

done on the morphology and structure and properties of α-Fe_2O_3 particles [11-13], however, work has not been done on nanostructured Fe_2O_3 films in polymer matrix by CBD. A variety of techniques have been used to fabricate iron oxide thin films such as pulsed laser deposition (PLD) [14], sol–gel [15], sputtering [16, 17], and molecular beam epitaxy (MBE) [18]. Compared to other deposition techniques, CBD offers the possibility of preparing small as well as large area coating of iron oxide thin films at low cost for various technological applications. Its low demand and simplicity make it very attractive. This paper reports on the investigations of the effects of variation of precursor concentration on the optical properties of the synthesized Fe_2O_3 films.

2. Experimental details

2.1 Synthesis of Iron Oxide Fe_2O_3 Films

Polyvinylpyrrolidon (PVP) solution was prepared by dissolving 4 grams of solid PVP in 400 cm^3 of distilled water. The mixture was stirred in a magnetic stirrer for about one hour until a homogeneous solution is obtained. This formed the polymer matrix. The glass microscopic slides which served as substrates were first degreased by dipping into a mixture of concentrated HCl and HNO_2 (Aqua-Regia) for about 30 hours. Next, they were scrubbed with soft rubber sponge in a cold detergent solution. Finally, they were rinsed in distilled water and dried in air. The degreased cleaned surfaces provided nucleation centers for growth of the films, thus producing highly adhesive uniform deposits. 100 cm^3 conical flasks used for preparation of the solution and 100 cm^3 beakers used as the chemical bath were thoroughly washed with detergent and rinsed with distilled water.

Several variations of bath constitutions of compounds whose films were to be deposited were prepared. The substrates were immersed vertically into the center of these baths, ensuring they neither touched the bottom nor the walls of the baths. For the experiments, the substrates were allowed to stay in the bath for different dip times to allow for optimum growth conditions and baths standardization. Synthetic rubber foam was used to cover the reaction bath protecting it from dust particles and other impurities and to suspend substrates into the bath. After deposition, the films were washed in distilled water and dried in air.

Five different baths (samples 4A – 4E) with varied concentrations of iron were prepared as follows: Sample 4A was obtained by mixing 0.010M $FeSO_4$, 60ml of PVP, 0.1M KCl and 2ml of 1M NaOH in a 100 cm^3 beaker. Samples 4B, 4C, 4D and 4E were obtained as in sample 4A, but with the concentration of $FeSO_4$ increased to 0.025M, 0.050M, 0.075M and 0.100M respectively. Substrates were then immersed in the baths of these samples and covered with synthetic foams. These were kept in an oven at 333K for six hours to allow for substantial deposits. After six hours, they were removed, rinsed in distilled water and annealed at 523K for two hours.

2.2 Characterization of Fe_2O_3 Thin Films

For structural characterization, the films were subjected to x-ray diffraction (XRD), in the range of scanning angle 2θ with Cukα radiation (λ = 1.5406Å) using Philips P.W 1500 X-ray diffractometer. The optical properties of the films were studied using absorption spectra in UV – VIS – NIR region obtained from Unico UV – 2102 PC spectrophotometer at normal incidence of light within the wavelength range 200nm – 1200nm.

3. Results and discussion

Figures 1(a) – 1(c) give the plots of absorbance, transmittance and reflectance against wavelengths for Fe_2O_3 films at varying concentrations, respectively. The absorption spectra for films with lower precursor concentration, fig. 1(a), show that these films have low absorbance < 20% in the UV-VIS-NIR regions, while that of the highest concentration absorbed highly ~35% in the UV-VIS region and decreased in the NIR region. It can be seen from this that absorption increased with concentration.

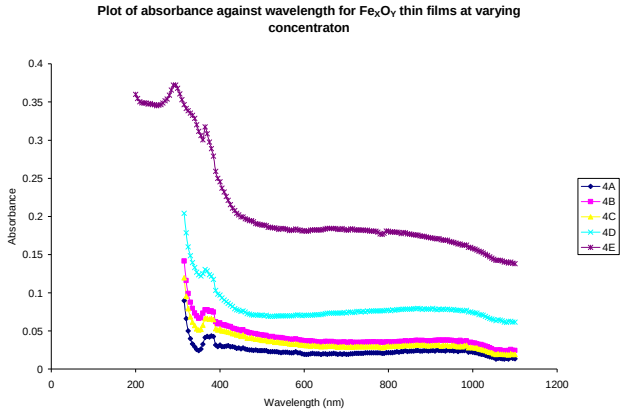

Fig 1(a): Absorption Spectra for Fe_2O_3 thin films

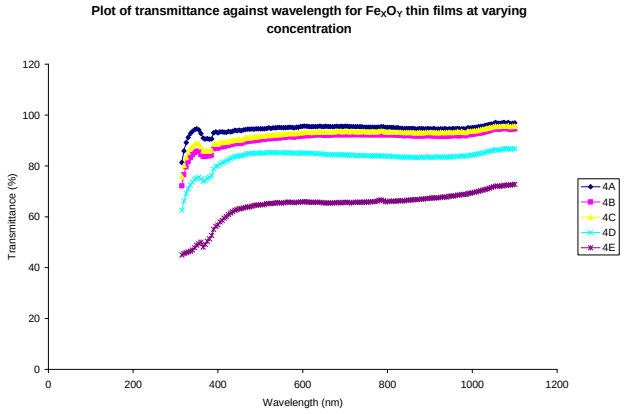

Fig 1(b): Transmittance Spectra for Fe_2O_3 thin films

The transmittance spectra given in fig 1(b) show that the films with lower concentration have high transmittance > 60% in the UV-VIS-NIR regions, while that with highest concentration has low transmittance ~40% in UV region but increased to > 60% in VIS-NIR regions. Here, transmittance can be seen to decrease with precursor concentration. The reflectance spectra given in fig 1(c) show that the reflectance of the films was low < 20% in the UV-VIS-NIR regions. Again this revealed that reflectance decreased with concentration.

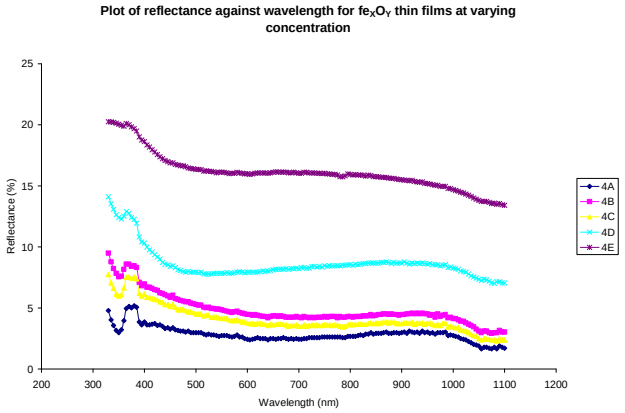

Fig 1(c): Reflectance Spectra for Fe_2O_3 thin films

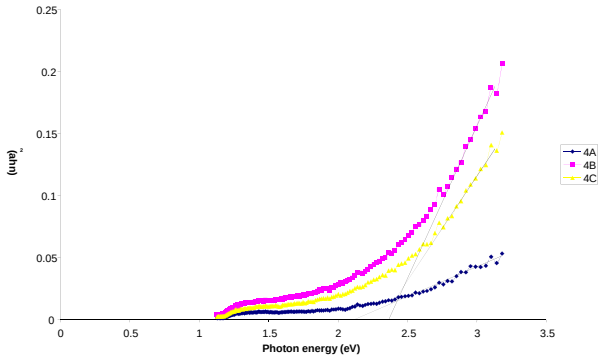

Fig 1(d): Band-gap Spectra for Fe_2O_3 thin films

The energy band-gaps of the films were determined from the relation between the absorption coefficient (α) and the incident photon energy (hν) given by [19] $\alpha = A\dfrac{\left(\alpha h\nu - E_g\right)^n}{h\nu}$; where A is a constant, E_g is the band gap energy of the material, and *n* depends on nature of transition. For direct allowed transition, n = ½; for direct forbidden transition, n = 3/2; and for indirect allowed transition, n = 2.

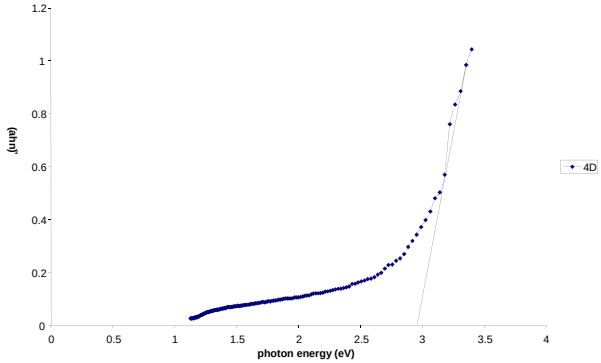

Fig 1(d): Band-gap Spectra for Fe_2O_3 thin films

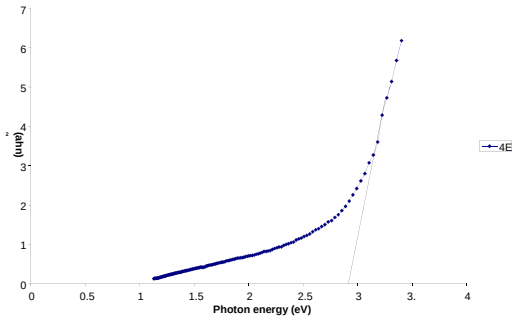

Fig 1(d): Band-gap Spectra for Fe_2O_3 thin films

The plots of $(\alpha h\nu)^n$ against $h\nu$ are given in fig 1(d). By extrapolating the straight portions of absorption coefficient $(\alpha h\nu)^n$ versus photon energy ($h\nu$) graphs to the point $(\alpha h\nu)^n = 0$, the band gaps were obtained from the intercepts since $E_g = h\nu$ when $(\alpha h\nu)^n = 0$. These values ranged from 2.10eV to 2.95eV. They agree fairly with those obtained by Ouertani et al [20] and Glasscock et al [21]. Band gap energy in the similar range (2.62 eV) for mechanically milled nanoparticles of Fe_2O_3 was also reported by Chakrabarti et al. [22]. The band gaps however did not show a consistent relationship with variation in precursor concentration. The plots of refractive index and absorption coefficient against photon energy of the Fe_2O_3 films are given by figs 1(e, f). From these graphs, it can be observed that both refractive index and absorption coefficient increased with precursor concentration. These parameters, for the highest concentration are much higher than the others. This may be attributed to the density of the films at this point. It can also be observed that both refractive index and absorption coefficient increased with radiation energy thus, making them suitable for application in optoelectronic devices. The refractive index was obtained from the relation $n = \frac{(1+R)^{1/2}}{(1-R)^{1/2}}$. Where R is the reflectance of the film. By determining the reflectance for any wavelength of radiation at normal incidence, the refractive index for that wavelength can be determined [23]. Absorption coefficient was obtained from $\alpha = \ln T^{-1} \times 10^6\ m^{-1}$. Where T is the transmittance of the film.

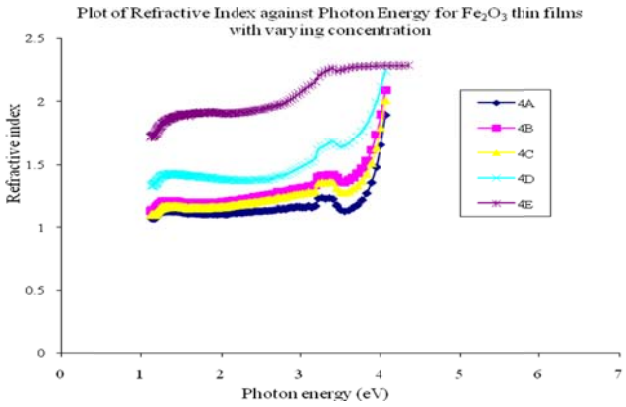

Fig 1(e): Refractive index Spectra for Fe_2O_3 thin films

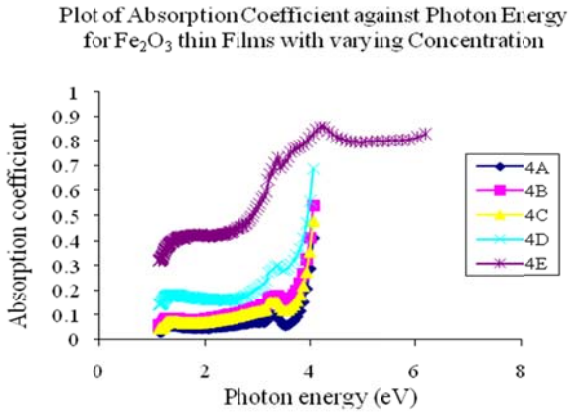

Fig 1(f): Absorption Coefficient Spectra for Fe_2O_3 thin films

Figs 1(g – i) give the XRD spectra for the synthesized Fe_2O_3 films with varying concentration. From fig. 1(g) which gives the spectra for film with precursor concentration (0.050M), peaks were obtained at 2θ = 20.67º, and 27.93º; corresponding to diffraction lines produced by (105), and (205) planes respectively.

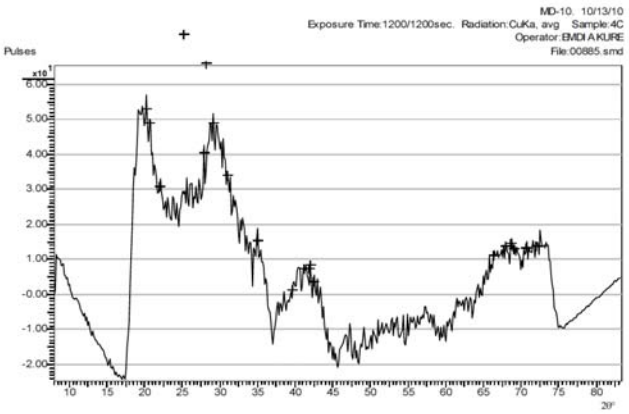

Fig 1(g): XRD diffractogram for Fe_2O_3 films with precursor concentration of 0.050M

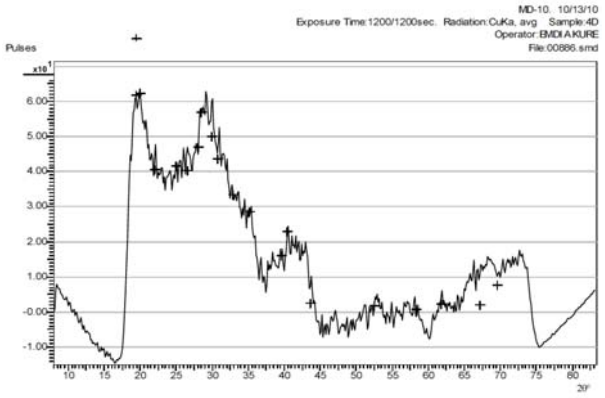

Fig 1(h): XRD diffractogram for Fe_2O_3 films with precursor concentration of 0.075M

Fig 1(i): XRD diffractogram for Fe_2O_3 films with precursor concentration of 0.100M

For fig. 1(h) which gives the spectra for film with precursor concentration (0.075M), peaks were obtained at 2θ = 27.00º and 40.50º; corresponding to diffraction lines produced by (205) and (316) planes respectively. Fig. 1(i) which gives the spectra for film with precursor

concentration (0.10M), show peaks at 2θ = 23.85º, 26.15º, and 33.95º, which corresponds to diffraction lines produced by (203), (116) and (109) planes respectively; these fairly agree with results obtained by Goyal et.al. [24] and Desai et.al. [25]. The XRD results also show that the films are nanocrystals of size 55.76nm; this size however decreased to 22.44nm when the precursor concentration was increased. The mean particle diameter of film 0.01M is 55.7nm, and that of film 0.1M is 22.44nm. The pH values of the solutions were 2.8 and 11.0, and 2.5 and 2.7, before and after addition of NaOH, respectively. These agree fairly with results obtained by Lu et al (1998) [26]. The size was determined using the Scherer's formula [27] given by $D = \frac{0.9\lambda}{\beta \cos\theta}$.

Where λ is wavelength of the x-ray, β is full width at half maximum (FWHM) of the peak with highest intensity and θ is the diffraction angle.

4. Conclusion

Nanostructured films of oxides of iron (Fe_2O_3), have been successfully synthesized using chemical bath deposition (CBD) technique and characterized using X-ray Diffraction (XRD). The structural composition of the films were determined and confirmed using XRD. The optical properties were studied using spectrophotometer. These films were observed to have low absorbance and reflectance of radiation in the ultraviolet, visible and near infra-red (UV-VIS-NIR) regions of optical spectra. These properties were found to increase with increase in concentration of precursor. They showed high transparency to radiation, which decreased with increase in precursor concentration in the VIS and NIR regions of optical spectra thus making them good materials for use in poultry roofs and walls. Some of the films have high band-gap which makes them suitable for a large variety of applications in microelectronic devices and optoelectronics; especially protective/ window coatings.

References

[1] R.M. Cornell, U. Schwertmann, The Iron Oxides, Second Ed.,Wiley-VCH, (2003), p. 11.
[2] R.N. Goyal et al., Materials Chemistry and Physics **116,** 638 (2009).
[3] A. A. Akl, Optical Properties of Crystalline and Non-Crystalline Iron Oxide Thin Films Deposited by Spray Pyrolysis, Applied Surface Science **233,** 307 (2004).
[4] R.K. Quinn, R.D. Nasby and R.J. Baughman, Mater.Res.Bull., **11,** lOll (1976).
[5] K.L. Hardee and A.J. Bard, J.EZectrochem. Soc. **123,** 1024 (1976).
[6] K. Itoh and J.O. M. Bockris, J.EZectrochem. SW. **131,** 1266 (1984).
[7] M. Jansen, H.P. Letschert, Nature **404,** 980 (2000).
[8] U. Bjorksten, J. Moser, M. Gratzel, Chem. Mater. **6,** 858 (1994).
[9] H. Hibst, Schwab E., in: R.W. Cahn, P. Hassen, E.J. Kramer (Eds.), Magnetic Recording Materials in Materials Science and Technology, vol. 3B, VCH Weinheim, 1994, p. 212.
[10] S. K.Bhar, N. Mukherjee, S. K. Maji, B. Adhikary, A. Mondal, Synthesis of Nanocrystalline Iron Oxide Ultrathin Films by Thermal Decomposition of Iron Nitropruside: Structural and Optical Properties, Materials Research Bulletin **45,** 1948 (2010).
[11] E. Matijecic, P. Scheiner, J. Colloid Interface Sci. **63,** 509 (1978).
[12] T. Jugimoto, A. Muramatsu, K. Sakata, D. Shindo, J. Colloid. Interface Sci. **158** (1993) 420.
[13] S.H. Kan, X.T. Zhang, S. Yu, D.M. Li, L.Z. Xiao, G.T. Zou, T.J. Li, W. Dong, Y.Z. Lu, J. Colloid, Interface Sci. **191**, 503 (1997).
[14] M.K. Krause, P. Esquinazi, M. Ziese, R. Hohne, A. Pan, A. Galkin, E. Zeldov, J. Magn. Magn. Mater. **245,** 1097 (2002).
[15] N.J. Tang, W. Zhong, H.Y. Jiang, X.L. Wu, W. Liu, Y.W. Du, J. Magn. Magn. Mater. **282,** 92 (2004).
[16] S. Ohta, A. Tterada, Thin Solid films **143,** 73 (1986).

[17] G. Zhang, C. Fan, L. Pan, F. Wang, P. Wu, H. Giu, Y. Gub, Y. Zhang, J. Magn. Magn. Mater. **293,** 737 (2005).
[18] W. Eerenstein, L. Kalev, L. Niesen, T.T.M. Palstra, T. Hibma, J. Magn. Magn. Mater. **73,** 258 (2003).
[19] J.I. Pankove, Optical Processes in Semiconductors Prentice-Hall, Inc. (1971)
[20] Ouertani, B., Ouerfelli, J., Saadoun, M., Ezzaouia, H., and Bessais, B., Characterization of Iron Oxide Thin Films Prepared From Spray Pyrolisis of Iron Trichloride-based Aqueous Solution. Thin Solid Films **516** (2008) 8584 – 8586.
[21] J.A. Glasscock, P.R.F. Barnes, I.C. Plumb, A. Bendavid, P.J. Martin, Structural, optical and electrical properties of undoped polycrystalline hematite thin films produced using filtered arc deposition, Thin Solid Films **516** (2008) 1716 – 1724
[22] M. Chakrabarti, A. Banerjee, D. Sanyal, M. Sutradhar, A. Chakrabarti, J. Mater. Sci. **43,** 4175 (2008).
[23] T.S. Robinson, Proc. Phys. Soc. London, **65B,** 910 (1952).
[24] R.N. Goyal, D. Kaur, A.K. Pandey, Growth and Characterization of Iron Oxide Nanocrystalline Thin Films Via Low-Cost Ultrasonic Spray Pyrolysis, Materials Chemistry and Physics **116,** 638 (2009).
[25] J.D. Desai, H.M. Pathan, S-K. Min, K-D. Jung, O-S. Joo, Preperation and Characterization of Iron Oxide Thin Films by Spray Pyrolysis using Methanolic and Ethanolic Solutions Applied Surface Science **252,** 2251 (2006).
[26]W. Lu, D. Yang, Y. Sun, Y. Guo, S. Xie, H. Li, Preparation and Structural Characterization of Nanostructured Iron Oxide Thin Films, Applied Surface Science **147,** 39 (1999).
[27] P.K. Ghosh, M.K. Mitra, and K.K. Chattopadhyay, ZnS Nanobelts Grown in a Polymer Matrix by Chemical Bath Deposition, Nanotechnology **16,** 107 (2005).